RSC Advances

PAPER

View Article Online
View Journal | View Issue

Cite this: *RSC Adv.*, 2016, **6**, 107776

A step towards the processability of insoluble or partially soluble functional and structural variants of polymers based on 3,4-alkylenedioxythiophene†

Bikash Kumar Sikder‡*

This work describes the processability of insoluble or partially soluble polymers based on 3,4-alkylenedioxythiophene (ADOT). Functional and structural variants of poly(3,4-alkylenedioxythiophene) (PADOTs), **P1(a–e)**, are synthesized, in which the side chain bulkiness was minimized to obtain better planarity and strong π-interaction. **P1(a–e)** were synthesized *via* chemical coupling polymerization using palladium acetate as the catalyst. Subsequent polymers structures (**P1a** to **P1e**) were obtained with either an enhanced alkylenedioxy bridge and or a side chain substituent in the alternate repeating units. Polymers **P1(a–c)** are insoluble in all common organic solvents, whereas the hydroxyl functional polymers **P1(d–e)** are soluble in organic polar solvents, which absorb at 535 nm and display optical properties both in solution and solid state. The conductivity of the oxidized thin films of the soluble polymers **P1d** and **P1e** is 4.7 S cm^{-1} and 1.5 S cm^{-1}, respectively. The neutral **P1(a–e)** polymers were dispersed in aqueous media using polystyrenesulfonate (PSS) and oxidized with sodium persulfate ($Na_2S_2O_8$). The particle size, stability and ion contents of these aqueous dispersions were characterized *via* various spectroscopic techniques. The thin films of the **P1(a–e)**:PSS dispersions were transparent with conductivity ranging from 8.1 × 10^{-2} to 1.2 × 10^{-2} S cm^{-1}. Spectroelectrochemical studies show that the **P1(a–e)**:PSS polymer films switch between opaque blue to a transmissive oxidized state with optical contrast in the range of 40–46%.

Received 15th August 2016
Accepted 24th October 2016

DOI: 10.1039/c6ra20592e

www.rsc.org/advances

Introduction

One class of conducting polymer that has seen significant attention from both academia and industry, largely because of its diverse and often remarkable properties, is poly(3,4-alkylenedioxythiophenes) (PADOTs), such as poly(3,4-ethylenedioxythiophene) (PEDOT) and poly(3,4-propylenedioxythiophene) (PProDOT). Their derivatives have been widely used in organic solar cells,[1] electrochromic devices,[2] chemical and biosensors,[3] fuel cells,[4] photovoltaic devices,[5] organic thin film transistors,[6] hole transport for light emitting diodes,[7] actuators[8] and antistatic coatings for cathode ray tubes.[9]

The interest in using PADOTs for the aforementioned applications is related to their low oxidation potentials, high transparency, they are conducting in the oxidized state, and exhibit excellent chemical and thermal stability.[10] Driven by the properties and uses of PADOTs, multiple lines of research are directed toward exploiting their processability and conductivity. Although the addition of bulky side chains ameliorates the processability of PADOTs, it invariably leads to reduced conductivity due to diminished intramolecular π–π interactions.[11] Conductivity is often associated with highly planar and strongly interacting π-conjugated polymers, whereas processability is typically associated with highly twisted and weakly interacting π-conjugated polymers, and hence it is difficult to achieve both properties simultaneously within a single material. Herein, polymers **P1(a–e)** are designed to achieve better π–π interactions by attaching less bulky groups on the side chain of the polymers.

Basically PADOTs are synthesized either by oxidative polymerization, which includes electrochemical polymerization,[12] chemical polymerization with a catalyst,[13] organic vapor phase polymerization,[14] solution casting polymerization,[15] and solid-state polymerization[16] or reductive polymerization, which is chemical coupling polymerization with a specified catalyst.[17] Chemical coupling reductive polymerization gives much better quality[18] materials in terms of their electrochemical properties, as well as it is an efficient method for large scale synthesis. For example Yamamoto *et al.*[19] investigated the conductivity of PEDOT, which was synthesized *via* oxidative polymerization[20]

Department of Chemistry, Indian Institute of Technology Bombay, Powai, Mumbai 400076, India. E-mail: bksikder@chem.iitb.ac.in; bksikder@uohyd.ac.in; Fax: +91 4023012460; Tel: +91 4023134808

† Electronic supplementary information (ESI) available: ^{1}H NMR, FTIR, GPC; solution doping and spectroelectrochemistry of the **P1e** polymer; dynamic light scattering plots, cyclic voltammogram, spectroelectrochemistry plots and optical switching plots of **P1a**:PSS, **P1b**:PSS, **P1c**:PSS and **P1e**:PSS. See DOI: 10.1039/c6ra20592e

‡ Present Address: Advanced Center for Research in High Energy Materials, University of Hyderabad, Hyderabad 500046, India.

and chemical coupling polymerization, over a certain range of temperature.[21] It was observed that the conductivity of iodine-doped PEDOT synthesized *via* the chemical coupling polymerization route was two hundred times greater than that of PEDOT prepared using the oxidative polymerization route. Hence, it is highly desirable to synthesize polymers using the chemical coupling polymerization method and later oxidized to obtain the doped form.

A series of reports by Reynolds and co-workers[22–25] on PADOTs have established that increasing the size of the alkylenedioxy bridge, Fig. 1: (I–III), or increasing the bulkiness of the substituent groups on the polymer backbone (V–VII), significantly enhances the optical contrast between the neutral and oxidized states by inducing an increased torsional twist in the conjugated system. Larger ring sizes and bulky substituents make more porous and open morphologies, which allow easy ingress and egress of ions during doping and dedoping mechanisms. This phenomenon is not only restricted to homopolymers, it is also relevant for copolymers and polymer blends. Hence, the **P1(a–e)** polymer structures were designed in a manner to increase the alkylenedioxy bridge along with restricted bulkiness on the polymer backbone (Scheme 1).

Most of the important applications or uses of PADOTs are in their conducting state. In order to make effective use of these polymers for varied applications it is essential that they are soluble or dispersible in their conducting state. The organic soluble PADOTs are generally soluble in organic solvents only in their non-conducting or reduced forms, whereas the corresponding conducting forms are insoluble. As a result, the potential use or versatility of use of these polymers is limited. Therefore, it is highly desirable to have PADOTs in the conducting form that can be processed either by dissolution or by dispersion in water. Unfortunately, relatively few viable technologies have emerged from the proof-of-concept stage to full commercial realization because of processability problems. In the 1980s Bayer AG[26] research laboratories developed emulsion polymerization of ethylenedioxythiophene (EDOT) in aqueous media in the presence of water soluble PSS, as charge-balancing dopant forming colloidal particles.[27] This combination resulted the random coil entanglement of PSS chains with PEDOT oligomers, which formed particles that consisted of a PEDOT-rich core covered by a PSS-rich shell. These aqueous colloidal solutions, poly(3,4-ethylenedioxythiophene)-poly(styrenesulfonate) (PEDOT:PSS), are quite successful and commercially available conducting polymers with nearly forty five different formulations under the trade name CLEVIOS P.[28] Unfortunately, the special nature of the commercially available PEDOT:PSS has some disadvantages. (1) It is based on a single monomer (EDOT) and hence no functional or structural variants are available. (2) Unreacted monomer or low molecular weight oligomers cannot be separated out of the mixture. (3) PSS, which is the charge-balancing dopant in PEDOT:PSS, desulfonates to release sulfuric acid on long standing.[29] Further, several research groups observed that the conductivity of PEDOT:PSS

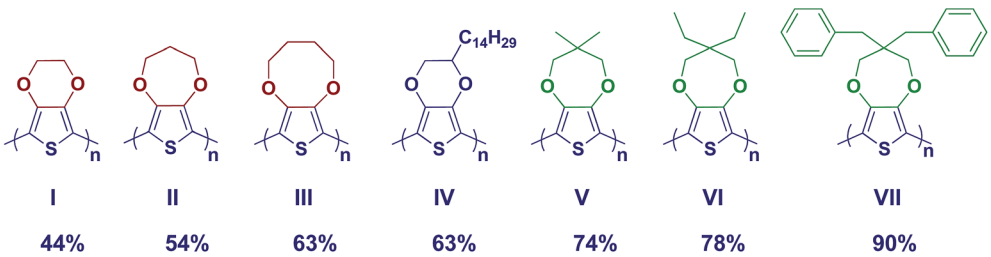

Fig. 1 Various PADOT structures with optical contrast.

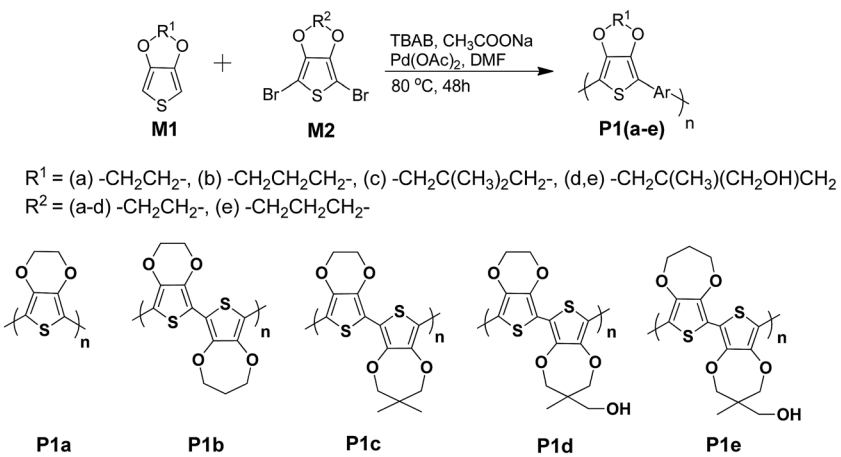

Scheme 1 Synthetic route for the preparation of the PADOTs.

increases more than thousand times upon the addition of compounds containing multiple hydroxyl groups[30] as a secondary dopant. In this article, the said lacunas in the commercially available PEDOT:PSS are addressed, such as structural variants of PADOTs, unreacted monomers and low molecular weight oligomers are removed during the workup of the polymers, the polymer dispersions can be prepared when required and finally the pendent hydroxyl group in the **P1d** and **P1e** polymers can itself act as a self-dopant for the polymers.

This report presents a collection of interconnected studies on PADOTs. Functional as well as structural variants of PADOTs are synthesized, where planarity and strong π-interaction were taken in account by restricting the bulkiness of the side chain. PADOTs were synthesized *via* the chemical coupling polymerization method using $Pd(OAc)_2$ as the catalyst[31] to obtain reduced or neutral polymers **P1(a–e)**. The introduction of hydroxyl groups along the polymer backbone results in functional dispersion as well as it addresses the issue of the addition of secondary dopants. Much attention is paid to developing a convenient and efficient method for preparing aqueous dispersions by dispersing powder polymers in suitable solvents, which can be processed when required to avoid the desulfonation caused by PSS on long standing.

Results and discussion

Polymers **P1(a–e)** were designed in a manner to induce enhancement in the dioxepine ring (**P1a** to **P1b** and **P1d** to **P1e**) or side chain bulkiness (**P1b** to **P1c** to **P1d**) in the alternate repeating units in the polymers. For the synthesis of the polymers, the monomers, **M1**, selected were either EDOT or ProDOT (or ProDOT derivatives), which were synthesized following reported procedures.[10,32,33] **M2** monomers were obtained by brominating EDOT or ProDOT using NBS.[33] 3,3-Dimethyl-3,4-dihydro-2*H*-thieno[3,4-*b*][1,4]dioxepine (ProDOT-Me_2) (structure V of Fig. 1), which has two methyl pendent groups on ProDOT, showed an optical contrast of 74%, and is the alternate repeating unit in polymer **P1c**. For polymers **P1d** and **P1e**, (3-methyl-3,4-dihydro-2*H*-thieno[3,4-*b*][1,4]dioxepin-3-yl)methanol (ProDOT-OH) is used as the alternate repeating unit, which can be easily synthesized in one step using the commercially available 3,4-dimethoxythiophene and 2-(hydroxymethyl)-2-methylpropane-1,3-diol. ProDOT-OH resembles the hydroxy derivate of ProDOT-Me_2 which introduces hydroxyl functionality along the backbone of polymers **P1d** and **P1e**. In summary, the subsequent polymers, **P1a** to **P1e**, were designed in a manner to increase the alkylenedioxy bridge in the alternate repeating units of the polymers (Scheme 1) or the bulkiness of the side chain (**P1b** to **P1d**).

General procedure for the synthesis of PADOT and its structural variants

In a flame dried two neck round bottom flask, under nitrogen atmosphere, equipped with a reflux condenser, 5 mmol of ADOT **M1(a–e)**, 5 mmol of tetrabutylammonium bromide (TBAB), 20 mmol of sodium acetate and 200 mL of anhydrous DMF were added and stirred at room temperature for 15 min followed by the addition of 5 mmol of 2,5-dibromo-ADOT **M2(a–b)** and 1 mol% of palladium acetate, and then heated to 80 °C for 48 h (Scheme 1). The color of the polymerization mixture turned to dark brown and purple for **P1(a–c)** and **P1(d–e)**, respectively, within a few minutes of the addition of the catalyst, which indicates the formation of polymers. These polymers were isolated by precipitating the reaction mixture in methanol. The resulting polymers were centrifuged and washed thoroughly with distilled methanol followed by stirring with hydrazine hydrate to obtain reduced (or neutral) polymers, and then washed thoroughly with water and dried under vacuum. The resulting polymers were isolated as a dark brown powder.

P1a, **P1b** and **P1c** were insoluble in all common organic solvents, whereas **P1d** and **P1e** were soluble in organic polar solvents, such as 1-methyl-2-pyrrolidone (NMP), *N*,*N*-dimethylformamide (DMF), dimethyl acetamide (DMAc) and dimethyl sulfoxide (DMSO). The soluble polymers **P1d** and **P1e** were purple in color when dissolved in DMSO and absorb at 535 nm, as shown in Fig. 2, which is typically associated with the π–π* transition in soluble ADOT based polymers.

FTIR spectra were recorded for polymers **P1(a–e)**. In the FTIR spectra of **P1(a–c)** (ESI†), the bands at 2925 cm^{-1} and 2855 cm^{-1} are due to the C–H stretching symmetric and asymmetric vibrations, respectively. The absorptions at 1645 cm^{-1} and 1445 cm^{-1} are associated to the C=C stretch of the thiophene ring. The bands at 1200 cm^{-1}, 1185 cm^{-1} and 1095 cm^{-1} are assigned to the C–O–C band stretching vibration in the alkylenedioxy ring. The absorptions at 985 cm^{-1}, 845 cm^{-1}, and 685 cm^{-1} are associated to the C–S stretching vibration. The soluble polymers, **P1d** and **P1e**, have primary hydroxyl groups which show a vibrational band at around 3400 cm^{-1} (ESI†). The bands at 2925 cm^{-1} and 2850 cm^{-1} are due to the C–H stretching symmetric and asymmetric vibrations, respectively. The absorptions at 1640 cm^{-1} and 1450 cm^{-1} are associated with the C=C stretch of the thiophene ring. The bands at 1290 cm^{-1} and 1125 cm^{-1} are assigned to the C–O–C band stretching vibration in the alkylenedioxy ring. The absorptions at 990 cm^{-1}, 850 cm^{-1}, and 690 cm^{-1} are due to the C–S stretching vibration.

Since polymers **P1d** and **P1e** are soluble only in high boiling solvents, Soxhlet purification could not be performed. ^1H NMR spectroscopy of **P1d** and **P1e** (ESI†) in DMSO-d_6 was performed to obtain well defined spectra, however a reasonable resolution

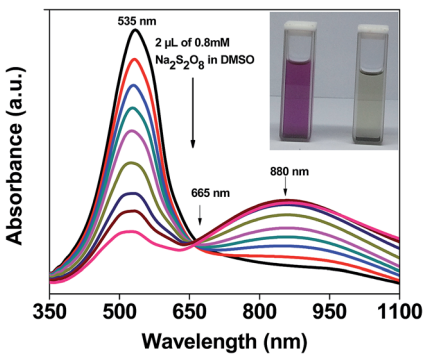

Fig. 2 Solution doping of **P1d** using 2 μL of 0.8 mM of $Na_2S_2O_8$ in DMSO with the isosbestic point at 665 nm.

could not be achieved. To obtain the molecular weight of the soluble polymers, gel permeable chromatography (GPC) experiments were performed on **P1d** and **P1e** using DMAc as the mobile phase. Unusually low molecular weights (M_w = 1000, PDI = 1.4) were observed for **P1d** and **P1e** probably because of absorption on the column due to the pendant hydroxyl group. This is in agreement with other cases of hydroxyl functional soluble conjugated polymers based on PADOTs.[33] Further, the polymeric nature of the organic soluble **P1d** and **P1e** polymers were characterized by solution doping, spectroelectrochemistry and conductivity studies. The insoluble polymers **P1a**, **P1b** and **P1c** were characterized *via* UV-vis absorption spectroscopy and spectroelectrochemically after dispersion in aqueous media.

For the solution doping study, the **P1d** and **P1e** polymers were reduced with hydrazine hydrate prior to the experiment, washed thoroughly with water and dried under vacuum. A series of UV-vis absorbance spectra were recorded as a function of concentration of dopant (0.8 mM solution of $Na_2S_2O_8$ in DMSO). In the reduced state, both the **P1d** and **P1e** solutions exhibited absorption at 535 nm corresponding to the π–π* transition, which imparts purple color to the solution (Fig. 2). The intensity of this peak decreases with an increase in the concentration of dopant. Moreover, an additional absorbance peak at 880 nm appeared upon the addition of the dopant. The absorbance at 880 nm indicates the formation of polaron charge carriers upon doping and the intensity of the peak at 880 nm increases with an increase in concentration of the dopant. An isosbestic point is observed at 665 nm for the peaks at 535 nm and 880 nm. Upon further addition of $Na_2S_2O_8$ solution the polymer achieved a highly doped state, which gave rise to a transparent solution (Fig. 2).

For spectroelectrochemical studies, thin films of **P1d** and **P1e** were coated on ITO-coated glass plates and used as the working electrode. A series of UV-vis spectra were then recorded as a function of applied potential in a 0.1 M solution of tetrabutylammoniumperchlorate (TBAP) in acetonitrile using silver wire as the reference electrode and platinum foil as the counter electrode. The **P1d** and **P1e** films were purple in colour at −1.0 V, and **P1d** absorbs at 560 nm, as seen in Fig. 3, which is due to the π–π* transition, whereas **P1e** exhibits two peaks with absorption maxima at 535 nm and 560 nm (ESI†). The splitting of the absorbance for **P1e** is due to vibronic coupling and is well documented in the literature.[22] Stepwise oxidation of the polymer showed a reduction in absorbance throughout the visible region as the color changes from the purple absorbing state (fully reduced form) to a highly transmissive state (oxidized form). The intensity of the absorbance at higher wavelength increases during the initial oxidation of the polymer, which is subsequently redshifted upon further oxidation of the polymer. This is attributed to the formation of a bipolaron and is in agreement with the other reported polymers based on ADOT derivatives.

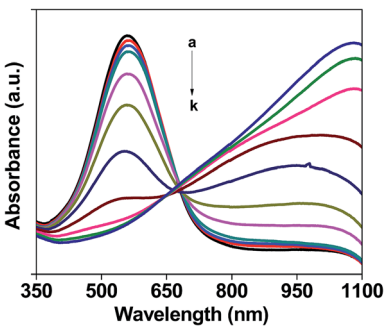

Fig. 3 Spectroelectrochemical spectra for **P1d** as a function of applied potential between −1 V and +1 V in 0.1 M TBAP/ACN: (a) −1, (b) −0.8, (c) −0.6, (d) −0.4, (e) −0.2, (f) 0, (g) +0.2, (h) +0.4, (i) +0.6, (j) +0.8 and (k) +1 V.

1% DMF solutions of **P1d** and **P1e** were prepared and spin coated on glass slides to obtain 100 nm thin films. The films were purple in color, however when baked at 150 °C, they turned light green color due to partial oxidation with atmospheric oxygen. The average conductivity of the partially oxidized **P1d** and **P1e** films was 6.2×10^{-3} S cm^{-1} and 6.6×10^{-3} S cm^{-1}, respectively. The partially oxidized **P1d** and **P1e** films were soaked in a 0.01 M chloroform solution of antimony pentachloride ($SbCl_5$) to obtain the oxidized form and were washed thoroughly with chloroform to remove traces of $SbCl_5$, dried and their conductivity measured. The conductivity of the oxidized **P1d** and **P1e** films was 4.7 S cm^{-1} and 1.5 S cm^{-1}, respectively. Hence the conductivity of the oxidized **P1d** and **P1e** thins films increased by three orders of magnitude compared to their neutral or partially oxidized form.

General procedure for the synthesis of aqueous dispersions of P1(a–e)

P1(a–c) are insoluble polymers, whereas **P1(d–e)** are soluble only in high boiling and polar solvents, which limits their processability. It is highly desirable to obtain the conducting form of conjugated polymers that can be processed either by dissolution or by dispersion in water. The processability issue of these polymers was circumvented by dispersing the **P1(a–e)** polymers of submicron particles using PSS in aqueous media. The common protocol followed for dispersing all five polymers is as follows: **P1** (1 g), PSS (M_w-2 lakh to 30 wt%) (1 g) and 100 mL of Milli Q water were mixed in a beaker and probe sonicated thrice for 30 minutes each time, which resulted in a brown colored emulsion with a reduced particle size. The **P1** polymers were oxidized with sodium persulfate ($Na_2S_2O_8$), and it was observed that 0.3 mole of $Na_2S_2O_8$ oxidizes 1 g of **P1**. Upon oxidation, the dispersion turned blue in color and the oxidized state of **P1** was confirmed *via* UV-vis spectroscopy. To achieve homogeneous micro-emulsions, the oxidized **P1** dispersions were further probe sonicated and finally passed through a homogenizer under varying pressure ranging from 800 bar to 1200 bar for 30 minutes. Then, the homogeneous dispersions obtained were treated twice with 20 g each of Amberlite IR-120 (strongly acidic cationic exchange resin) and Amberlite IRA-410 (strongly basic anionic exchange resin) to eliminate the inorganic ions present in the dispersions, which resulted in dispersions of p-type conductive polymer **P1** and polyanion PSS in aqueous media.

Characterization of P1(a–e):PSS aqueous dispersions

UV-visible absorption spectroscopy. The oxidized state of the **P1(a–e)** polymer dispersions were confirmed by UV-vis absorbance spectroscopy. Absorbance maxima at 790 nm were observed for **P1a** and **P1b**, whereas the maxima for **P1(c–e)** were observed above 900 nm (Fig. 4(a)), which are the features typically seen in the doped state of polymers based on ADOT. When these dispersions were reduced with hydrazine hydrate, the absorption maxima were shifted in the range of 550–600 nm (Fig. 4(b)), which is ascribed to the π–π^* electronic transition of the reduced state of the **P1(a–e)** polymers.

Particle size of P1(a–e):PSS dispersions. Dynamic light scattering (DLS) experiments were performed at an average count rate of 100–170 kcps (kilo counts per second), and a polydispersity of 0.2–0.25. The optimal concentration for DLS measurement was evaluated over a range of concentrations to yield the best signal possible. The dispersion concentration used (1 mL was diluted to 10 mL with MilliQ water) resulted in the highest measurable signal, and an increase in the polymer concentration resulted in total absorption and extinguishing of the scattered light. The temperature was kept constant (295 K) in the surrounding decalin (filtered through a Whatman Anopore syringe filter of 0.45 μm). The scattered light was collected at 90° from the incident laser. Using the DLS software, the hydrodynamic diameter (D_h) was calculated and weighted in relation to the number of particles in the samples. The mean D_h was calculated to be 430 nm, 454 nm, 470 nm, 306 nm and 330 nm for the **P1a**, **P1b**, **P1c**, **P1d** and **P1e** dispersions, respectively, based on five average readings. The figures are shown in the ESI.† It is evident that the hydrodynamic diameter of the hydroxyl functional polymers dispersions **P1d** and **P1e** are 100 nm smaller in that of the un-functional polymer **P1a**, **P1b** and **P1c** dispersions. However, DLS measured the hydrodynamic diameter (containing water molecules), and hence the final features are smaller. The exact particle size was confirmed by performing field emission gun transmission electron microscopy (FEG-TEM). Fig. 5 presents a representative FEG-TEM micrograph of the **P1d** particles, in which the particles resemble irregular shells with a thickness of 10–15 nm.

Stability of P1(a–e):PSS dispersions. Zeta potential experiments were performed to determine the stability of the polymer dispersions. Zeta potential experiments were recorded with respect to the pH of the dispersions at 25 °C. The optimal concentration for zeta potential measurement was evaluated over a range of concentrations to yield the best signal possible. The dispersion concentration used (1 mL was diluted to 3 mL with Milli Q water) resulted in the highest measurable signal. The zeta potential value of a moderately stable dispersion is in the range of ±30 mV to ±40 mV. The zeta potential values of **P1a**, **P1b**, **P1c**, **P1d** and **P1e** were found to be −31.7 mV, −33.2 mV, −34.8 mV, −35.1 mV and −32.68 mV, respectively, which evidently indicate that the dispersions have moderate stability.

Ion content of P1(a–e):PSS dispersions. To determine the content of palladium and sodium ions present in the dispersions, inductive coupled plasma atomic emission spectroscopy was performed. Standard solutions of the ions of interest were prepared by diluting commercial standards, and the calibration was linear with an error of 1%. Palladium and sodium ions are characterized by very strong emission, and their content in the final dispersion was found to be 0.7 ppm and 1.6 ppm, respectively.

Conductivity of P1(a–e):PSS dispersions. The **P1(a–e)** dispersions were spin coated on glass slides to obtain transparent thin films and their conductivity was measured. The conductivity of the **P1(a–e)** films were found to be in the range of 8.1×10^{-2} S cm^{-1} to 1.2×10^{-2} S cm^{-1}. A sample of the commercially available PEDOT:PSS showed a conductivity of 2.3×10^{-2} S cm^{-1} under identical conditions. It should however

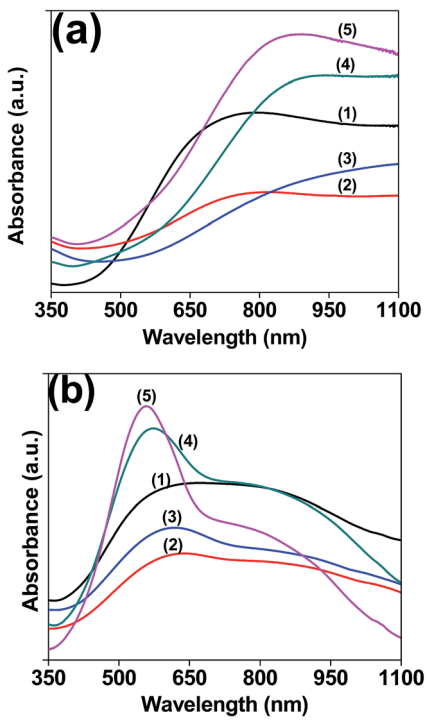

Fig. 4 UV-vis spectra of (a) (1) **P1a**, (2) **P1b**, (3) **P1c**, (4) **P1d** and (5) **P1e**. (b) Hydrazine hydrate treated (1) **P1a**, (2) **P1b**, (3) **P1c**, (4) **P1d** and (5) **P1e** aqueous dispersions.

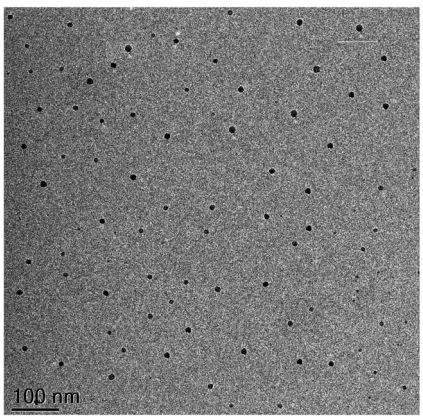

Fig. 5 FEG-TEM image of **P1d** particles.

be noted that higher conductivity values for CLEVIOS P have been reported elsewhere[34] and that combined chemical and thermal treatment can give much higher conductivities.

Electrochemical P1(a–e):PSS dispersion studies. The **P1(a–e)** dispersions were spin coated on ITO-coated glass slides and were used as working electrodes for the electrochemical studies. For cyclic voltammetry, Ag/Ag^+ was used as the reference electrode and platinum foil as the counter electrode. Cyclic voltammetric studies of the polymer films were performed in 0.1 M TBAP in acetonitrile by cycling the potential between −0.60 V and +1.20 V at a scan rate of 25 mV s^{-1}, 50 mV s^{-1}, 75 mV s^{-1}, 100 mV s^{-1}, 125 mV s^{-1} and 150 mV s^{-1}. At the scan rate of 150 mV s^{-1}, the oxidation peaks were in the range of +0.02 V to +0.74 V and the corresponding reduction peaks were in the range of −0.34 V to +0.23 V *vs.* the Ag/Ag^+ reference electrode for the **P1(a–e)** polymers. The cyclic voltammogram of **P1d** shown in Fig. 6 represents a positive shift in the oxidation potential at higher scan rates, which compensates the charge transfer resistance. The scan rate dependence study indicates the linearity (R^2 value of the lines are in the range of 0.984–0.998) of current as a function of square root of the scan rate, as shown in Fig. 7, which suggests a diffusion-limited redox process.[35]

For the spectroelectrochemical studies, a series of UV-vis spectra were obtained as a function of applied potential in a 0.1 M solution of TBAP in acetonitrile using silver wire as the reference electrode and platinum foil as the counter electrode. The spectroelectrochemical spectra of **P1(a–e)** are similar with respect to the growth of the oxidation peak as a function of applied positive potential. The polymer films were opaque blue at −1.0 V and exhibited absorption maxima at 525 nm, 540 nm, 585 nm, 580 nm and 555 nm for **P1a**, **P1b**, **P1c**, **P1d** and **P1e**, respectively, which are assigned to the π–π* transition. Fig. 8 presents the spectroelectrochemical spectra of **P1d**, in which stepwise oxidation of the polymer resulted in a reduction in absorbance throughout the visible region since the color changes from the dark blue absorbing state (fully reduced form) to a highly transmissive state (oxidized form). The interesting feature to note in Fig. 8 is the growth of the oxidized peak at 950 nm, which is ascribed to the polaron charge carriers. The intensity of this peak increases during the initial oxidation of the polymer but later on the intensity becomes saturated, even upon further oxidation of the polymer. This is ascribe to the formation of bipolarons and is in agreement with other reported polymers based on 3,4-propylenedioxythiophene derivatives.[32] The optical contrast of the **P1(a–e)** films was calculated from the difference in % *T* between the completely oxidized and reduced state, which was found to be 40–46%. For optical switching studies, **P1(a–e)** films were switched at 525 nm, 540 nm, 585 nm, 580 nm and 555 nm for **P1a**, **P1b**, **P1c**, **P1d** and **P1e**, respectively, by repeated potential steps between their reduced (−1.0 V) and oxidized (+1.0 V) states in a 0.1 M solution of TBAP in acetonitrile, using silver wire as the reference electrode and platinum foil as the counter electrode. Fig. 9 presents the optical switching spectra of the **P1d** thin film, which was switched at 580 nm and was monitored as a function of time. The switching of the film was carried out by switching the potential between −1.0 V and +1.0 V with a delay time of 3 s while monitoring the % *T* of the polymer at its λ_{max}. The contrast calculated from the difference in % *T* between the completely reduced and oxidized state was 40%, 42%, 42%, 44% and 46% for **P1a**, **P1b**, **P1c**, **P1d** and **P1e**, respectively.

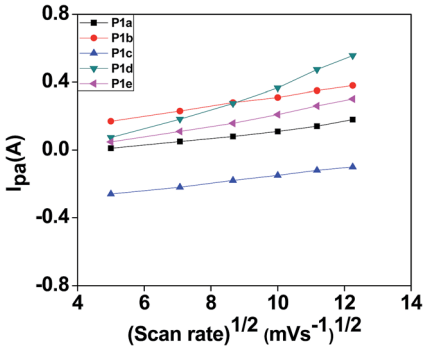

Fig. 7 Square root of scan rate *vs.* anodic current peak of the redox process for **P1(a–e)**.

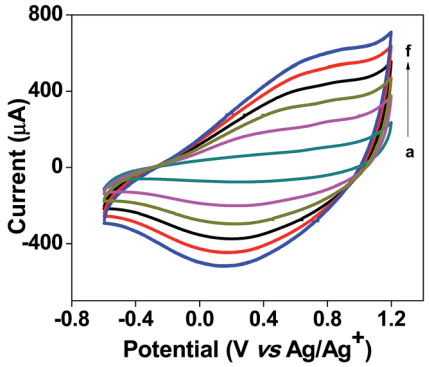

Fig. 6 Cyclic voltammogram of **P1d** in 0.1 M TBAP at a scan rate of (a) 25 mV s^{-1}, (b) 50 mV s^{-1}, (c) 75 mV s^{-1}, (d) 100 mV s^{-1}, (e) 125 mV s^{-1} and (f) 150 mV s^{-1}.

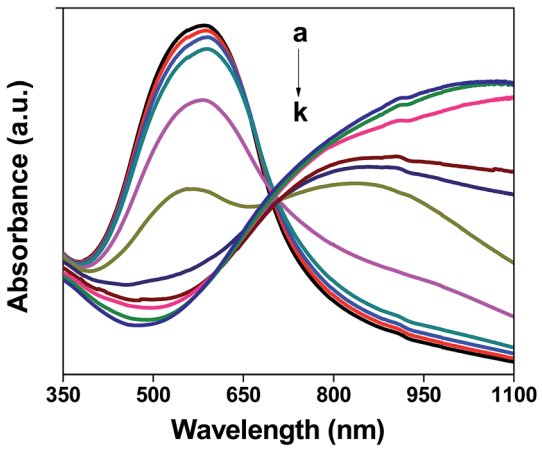

Fig. 8 Spectroelectrochemical spectra of **P1d** as a function of applied potential between −1 V and +1 V in 0.1 M TBAP/ACN: (a) −1, (b) −0.8, (c) −0.6, (d) −0.4, (e) −0.2, (f) 0, (g) 0.2, (h) 0.4, (i) 0.6, (j) 0.8 and (k) 1 V.

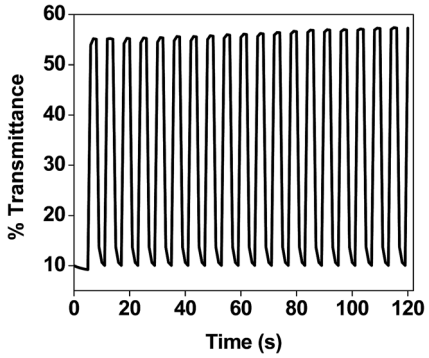

Fig. 9 Optical switching studies for **P1d** film deposited by spin coating and monitored at 580 nm, when stepped between its reduced (−1.0 V) and oxidized (+1.0 V) state.

Conclusions

Herein, the synthesis and processability of functional and structural variants of polymers based on 3,4-alkylenedioxythiophenes are discussed. The primary focus was on the subsequent synthesis of PADOT polymers to achieve better π-stacking, increase the alkylenedioxy bridge ring size and introduce hydroxyl functional groups. The **P1(a–e)** polymers were prepared *via* the chemical coupling reductive polymerization method using $Pd(OAc)_2$ as the catalyst, and were obtained in powder form. **P1(a–c)** are insoluble, whereas the hydroxyl functional polymers **P1d** and **P1e** are soluble in organic solvents and display optically properties both in solution and solid state and are conducting in their oxidized state. Aqueous dispersions were developed to overcome the processability issue of insoluble or partially soluble polymers based on ADOT. Sub-micron particles of PADOTs were dispersed in aqueous media using a counter anionic surfactant. The dispersions particle size, ion content, stability and conductivity were measured using various techniques. Thin films of these dispersions are transparent and conducting in the oxidized state. The electro-optical properties of the dispersions were investigated using spectroelectrochemical studies.

Experimental section

Instrumentation and methods

^{1}H NMR spectroscopy was recorded using a BRUKER 400 MHz NMR spectrometer. Fourier transform infrared spectroscopy (FTIR) experiments were performed on a Perkin-Elmer Spectrum One FTIR-SPECTROMETER using an NaCl window. Gel permeation chromatography (GPC, Waters 515 HPLC) was performed with an RI detector (Waters 2414) using HPLC grade dimethylacetamide (DMAc) as the mobile phase. **P1d** and **P1e** solutions in DMAc of concentration 1.0 mg mL^{-1} were injected in the GPC column (Styragel HR2 DMAc) at a flow rate of 0.4 mL min^{-1}. Narrow molecular weight distribution polystyrene standards (Polymer Standards Service) with a polydispersity index ≤ 1.1 were used for the GPC molecular weight calibration. UV-visible spectra were recorded with a Perkin-Elmer Lambda 35 UV/vis spectrometer, and corrected for baseline with a solvent-filled cuvette. Dynamic light scattering (DLS) experiments were conducted using a BI-200SM motor-driven goniometer, BI-9000AT digital auto-correlator and BI-9025AT photon counter system (Brookhaven Instruments Corporation, USA). Zeta potential was measured using a Zetasizer Ver. 6.01 (Malvern Instruments Ltd). Field emission gun transmission electron microscopy (FEG-TEM) measurements were carried out on a JEOL JEM2100F field emission electron microscope operated at 120 kV. Inductively coupled plasma-atomic emission spectrometry (ICP-AES) experiments were conducted using a SPECTRO ARCOS (Spectro, Germany). Sheet resistance was measured using a four-point probe (Lucas Labs Pro4, Lucas-Signatone) connected to a Keithly 2400 source-meter (Cleveland, OH, USA). Electrochemical measurements were performed with a CH Instruments CHI-760 workstation potentiostat controlled with a PC. For cyclic voltammetry characterization, Pt foil was used as the counter electrode and Ag/Ag$^+$ as reference electrodes and for spectroelectrochemistry and optical switching Pt foil was used as the counter electrode and Ag wire as the reference electrode. ITO-coated glass slides were used as the working electrode. For optical switching studies an EG&G PAR Model 273 potentiostat/galvanostat was used to control the potential.

Materials

Monomers 3,4-ethylenedioxythiophene (EDOT), 3,4-propylenedioxythiophene (ProDOT), 3,3-dimethyl-3,4-dihydro-2*H*-thieno[3,4-*b*][1,4] dioxepine (ProDOT-Me_2), 2,5-dibromo-3,4-ethylenedioxythiophene (DBEDOT), 2,5-dibromo-3,4-propylenedioxythiophene (DBProDOT) and (3-methyl-3,4-dihydro-2*H*-thieno[3,4-*b*][1,4]dioxepin-3-yl) methanol (ProDOTOH) were synthesized according to a reported procedure. Tetrabutylammonium bromide (TBAB), sodium acetate, sodium persulfate, acetonitrile and anhydrous *N*,*N*-dimethylformamide were purchased from Merck. Palladium acetate, tetrabutylammoniumperchlorate (TBAP) and antimony pentachloride ($SbCl_5$) were purchased from Aldrich. Indium-doped tin oxide (ITO)-coated glass slides were obtained from Delta Technologies.

Conflict of interest

The authors declare no competing financial interests.

Acknowledgements

Author acknowledges Council of Scientific and Industrial Research, India, for financial support. Department of Chemistry, Indian Institute of Technology Bombay, India for providing infrastructure and Prof. Tushar Jana for sharing his pearls of wisdom and comments that greatly improved the manuscript.

References

1 (*a*) D. H. Kim, S. E. Atanasov, P. Lemaire, K. Lee and G. N. Parsons, *ACS Appl. Mater. Interfaces*, 2015, **7**, 3866; (*b*)

F. C. Krebs, S. A. Gevorgyan and J. Alstrup, *J. Mater. Chem.*, 2009, **19**, 5442; (*c*) H. Xu, X. Zhang, C. Zhang, Z. Liu, X. Zhou, S. Pang, X. Chen, S. Dong, Z. Zhang, L. Zhang, P. Han, X. Wang and G. Cui, *ACS Appl. Mater. Interfaces*, 2012, **4**, 1087; (*d*) S. Na, G. Wang, S. Kim, T. Kim, S. Oh, B. Yu, T. Lee and D. Kim, *J. Mater. Chem.*, 2009, **19**, 9045.

2 (*a*) P. Andersson, R. Forchheimer, P. Tehrani and M. Berggren, *Adv. Funct. Mater.*, 2007, **17**, 3074; (*b*) R. J. Mortimer, A. L. Dyer and J. R. Reynolds, *Displays*, 2006, **27**, 2.

3 (*a*) D. T. McQuade, A. E. Pullen and T. M. Swager, *Chem. Rev.*, 2000, **100**, 2537; (*b*) J. Park, H. K. Kim and Y. Son, *Sens. Actuators, B*, 2008, **133**, 244; (*c*) A. Michalska and K. Maksymiuk, *Anal. Chim. Acta*, 2004, **523**, 97; (*d*) L. Setti, A. Fraleoni-Morgera, B. Ballarin, A. Filippini, D. Frascaro and C. Piana, *Biosens. Bioelectron.*, 2005, **20**, 2019.

4 (*a*) B. Winther-Jensen, K. Fraser, C. Ong, M. Forsyth and D. R. MacFarlane, *Adv. Mater.*, 2010, **15**, 1727; (*b*) B. Winther-Jensen, O. Winther-Jensen, M. Forsyth and D. R. MacFarlane, *Science*, 2008, **5889**, 671; (*c*) M. C. Lefebvre, Z. Qi and P. G. Pickup, *J. Electrochem. Soc.*, 1999, **146**, 2054.

5 (*a*) E. Nasybulin, S. Wei, M. Cox, I. Kymissis and K. Levon, *J. Phys. Chem. C*, 2011, **115**, 4307; (*b*) A. C. Arias, M. Granström, D. S. Thomas, K. Petritsch and R. H. Friend, *Phys. Rev. B: Condens. Matter Mater. Phys.*, 1999, **60**, 1854; (*c*) A. C. Arias, M. Granström, K. Pertritsch and R. H. Friend, *Synth. Met.*, 1999, **102**, 953; (*d*) G. P. Kushto, W. Kim and Z. H. Kafafi, *Appl. Phys. Lett.*, 2005, **86**, 093502.

6 (*a*) H. Sirringhaus, T. Kawase, R. H. Friend, T. Shimoda, M. Inbasekaran, W. Wu and E. P. Woo, *Science*, 2000, **290**, 2123; (*b*) M. Halik, H. Klauk, U. Zschieschang, T. Kriem, G. Schmid, W. Radlik and K. Wussow, *Appl. Phys. Lett.*, 2002, **81**, 289.

7 (*a*) M. Granström, M. Berggren and O. Inganäs, *Science*, 1995, **267**, 1479; (*b*) N. R. Armstrong, W. Wang, D. M. Alloway, D. Placencia, E. Ratcliff and M. Brumbach, *Macromol. Rapid Commun.*, 2009, **30**, 717.

8 (*a*) F. Vidal, C. Plesse, G. Palaprat, A. Kheddar, J. Citerin, D. Teyssiè and C. Chevrot, *Synth. Met.*, 2006, **156**, 1299; (*b*) H. Okuzaki, H. Suzuki and T. Ito, *Synth. Met.*, 2009, **159**, 2233.

9 F. Jonas and J. T. Morrison, *Synth. Met.*, 1997, **85**, 1397.

10 (*a*) L. Groenendaal, F. Jonas, D. Freitag, H. Pielartzik and J. R. Reynolds, *Adv. Mater.*, 2000, **12**, 481; (*b*) L. B. Groenendaal, G. Zotti, P.-H. Aubert, S. M. Waybright and J. R. Reynolds, *Adv. Mater.*, 2003, **15**, 855; (*c*) S. Kirchmeyer and K. Reuter, *J. Mater. Chem.*, 2005, **15**, 2077; (*d*) M. Salsamendi, J. Abad, R. Marcilla, C. Pozo-Gonzalo, A. Urbina, H. Grande, J. Colchero and D. Mecerreyes, *Polym. Adv. Technol.*, 2011, **22**, 1665.

11 J. Roncali, *Chem. Rev.*, 1992, **92**, 711.

12 (*a*) R. Asami, M. Atobe and T. Fuchigami, *J. Am. Chem. Soc.*, 2005, **127**, 13160; (*b*) J. Heinze, B. A. Frontana-Uribe and S. Ludwigs, *Chem. Rev.*, 2010, **110**, 4724; (*c*) N. K. Sadanandhan, S. J. Devaki, R. K. Narayanan and M. Cheriyathuchenaaramvalli, *ACS Appl. Mater. Interfaces*, 2015, **7**, 18028; (*d*) R. Xiao, S. I. Cho, R. Liu and S. B. Lee, *J. Am. Chem. Soc.*, 2007, **129**, 4483; (*e*) R. C. Shallcross, G. D. D'Ambruoso, J. Pyun and N. R. Armstrong, *J. Am. Chem. Soc.*, 2010, **132**, 2622.

13 (*a*) R. H. Karlsson, A. Herland, M. Hamedi, J. A. Wigenius, A. Åslund, X. Liu, M. Fahlman, O. Inganäs and P. Konradsson, *Chem. Mater.*, 2009, **21**, 1815; (*b*) S. Nagarajan, J. Kumar, F. F. Bruno, L. A. Samuelson and R. Nagarajan, *Macromolecules*, 2008, **41**, 3049; (*c*) V. Rumbau, J. A. Pomposo, A. Eleta, J. Rodriguez, H. Grande, D. Mecerreyes and E. Ochoteco, *Biomacromolecules*, 2007, **8**, 315; (*d*) X. Zhang, J. Lee, G. S. Lee, D. Cha, M. J. Kim, D. J. Yang and S. K. Manohar, *Macromolecules*, 2006, **39**, 470.

14 (*a*) A. Ugur, F. Katmis, M. Li, L. Wu, Y. Zhu, K. K. Varanasi and K. K. Gleason, *Adv. Mater.*, 2015, **27**, 4604; (*b*) H. Goktas, X. Wang, A. Ugur and K. K. Gleason, *Macromol. Rapid Commun.*, 2015, **36**, 1283; (*c*) S. Lee and K. K. Gleason, *Adv. Funct. Mater.*, 2015, **25**, 85; (*d*) S. Lee, D. C. Paine and K. K. Gleason, *Adv. Funct. Mater.*, 2014, **24**, 7187; (*e*) J. P. Lock, S. G. Im and K. K. Gleason, *Macromolecules*, 2006, **39**, 5326; (*f*) H. Chelawat, S. Vaddiraju and K. Gleason, *Chem. Mater.*, 2010, **22**, 2864.

15 (*a*) B. Winther-Jensen, D. W. Breiby and K. West, *Synth. Met.*, 2005, **152**, 1; (*b*) J. Kim, J. You, B. Kim, T. Park and E. Kim, *Adv. Mater.*, 2011, **23**, 4168; (*c*) J. U. Lind, T. S. Hansen, A. E. Daugaard, S. Hvilsted, T. L. Andresen and N. B. Larsen, *Macromolecules*, 2011, **44**, 495; (*d*) R. Allen, L. Pan, G. G. Fuller and Z. Bao, *ACS Appl. Mater. Interfaces*, 2014, **6**, 9966.

16 (*a*) N. Gulprasertrat, J. Chapromma, T. Aree and Y. Sritana-anant, *J. Appl. Polym. Sci.*, 2015, **132**(28), 42233; (*b*) F. Wu, Z. Xu, Y. Wang and M. Wang, *RSC Adv.*, 2014, **4**, 38797; (*c*) X. Yin, F. Wu, N. Fu, J. Han, D. Chen, P. Xu, M. He and Y. Lin, *ACS Appl. Mater. Interfaces*, 2013, **5**, 8423; (*d*) H. Meng, D. F. Perepichka, M. Bendikov, F. Wudl, G. Z. Pan, W. Yu, W. Dong and S. Brown, *J. Am. Chem. Soc.*, 2003, **125**, 15151; (*e*) H. Meng, D. F. Perepichka and F. Wudl, *Angew. Chem., Int. Ed.*, 2003, **42**, 658.

17 (*a*) C. R. G. Grenier, S. J. George, T. J. Joncheray, E. W. Meijer and J. R. Reynolds, *J. Am. Chem. Soc.*, 2007, **129**, 10694; (*b*) H. Zhao, B. Zhu, J. Sekine, S. Luo and H. Yu, *ACS Appl. Mater. Interfaces*, 2012, **4**, 680; (*c*) T. W. Holcombe, C. H. Woo, D. F. J. Kavulak, B. C. Thompson and J. M. J. Fréchet, *J. Am. Chem. Soc.*, 2009, **131**, 14160; (*d*) D. M. Welsh, L. J. Kloeppner, L. Madrigal, M. R. Pinto, B. C. Thompson, K. S. Schanze, K. A. Abboud, D. Powell and J. R. Reynolds, *Macromolecules*, 2002, **35**, 6517.

18 (*a*) Y. Zhang, K. Tajima, K. Hirota and K. Hashimoto, *J. Am. Chem. Soc.*, 2008, **130**, 7812; (*b*) H. D. Magurudeniya, P. Sista, J. K. Westbrook, T. E. Ourso, K. Nguyen, M. C. Maher, M. G. Alemseghed, M. C. Biewer and M. C. Stefan, *Macromol. Rapid Commun.*, 2011, **32**, 1748; (*c*) L. Wen, B. C. Duck, P. C. Dastoor and S. C. Rasmussen, *Macromolecules*, 2008, **41**, 4576; (*d*) R. S. Loewe, S. M. Khersonsky and R. D. McCullough, *Adv. Mater.*, 1999, **11**, 250.

19 T. Yamamoto, M. Abla, T. Shimizu, D. Komarudin, B. Lee and E. Kurokawa, *Polym. Bull.*, 1999, **42**, 321.
20 M. Granström and O. Inganäs, *Adv. Mater.*, 1995, **7**, 1012.
21 T. Yamamoto, D. Komarudin, M. Arai, B. Lee, H. Suganuma, N. Asakawa, Y. Inoue, K. Kubota, S. Sasaki, T. Fukuda and H. Matsuda, *J. Am. Chem. Soc.*, 1998, **120**, 2047.
22 (*a*) A. Kumar, D. M. Welsh, M. C. Morvant, F. Piroux, K. A. Abboud and J. R. Reynolds, *Chem. Mater.*, 1998, **10**, 896; (*b*) D. M. Welsh, A. Kumar, E. W. Meijer and J. R. Reynolds, *Adv. Mater.*, 1999, **11**, 1379.
23 (*a*) C. L. Gaupp, D. M. Welsh and J. R. Reynolds, *Macromol. Rapid Commun.*, 2002, **23**, 885; (*b*) C. L. Gaupp, D. M. Welsh, R. D. Rauh and J. R. Reynolds, *Chem. Mater.*, 2002, **14**, 3964.
24 (*a*) I. Schwendeman, C. L. Gaupp, J. M. Hancock, L. Groenendaal and J. R. Reynolds, *Adv. Funct. Mater.*, 2003, **13**, 541; (*b*) G. Sönmez, I. Schwendeman, P. Schottland, K. Zong and J. R. Reynolds, *Macromolecules*, 2003, **36**, 639.
25 (*a*) K. Krishnamoorthy, A. V. Ambade, M. Kanungo, A. Q. Contractor and A. Kumar, *J. Mater. Chem.*, 2001, **11**, 2909; (*b*) K. Krishnamoorthy, M. Kanungo, A. Q. Contractor and A. Kumar, *Synth. Met.*, 2001, **124**, 471.
26 (*a*) A. G. Bayer, Eur. Patent, 440957, 1991; (*b*) A. G. Bayer, Eur. Patent, 339340, 1988.
27 I. Winter, C. Reece, F. Hormes, G. Heywang and F. Jonas, *Chem. Phys.*, 1995, **194**, 207.
28 Commercially available under trade name "Clevios-P", http://www.heraeus-clevios.com/en/products/heraeus-conductive-polymers-products.aspx.
29 X. H. Yang, F. Jaiser, B. Stiller, D. Neher, F. Galbrecht and U. Scherf, *Adv. Funct. Mater.*, 2006, **16**, 2156.
30 (*a*) A. M. Nardes, R. A. J. Janssen and M. A. Kemerink, *Adv. Funct. Mater.*, 2008, **18**, 865; (*b*) J. Ouyang, Q. Xu, C. Chu, Y. Yang, G. Li and J. Shinar, *Polymer*, 2004, **45**, 8443; (*c*) X. Crispin, F. L. E. Jakobsson, A. Crispin, P. C. M. Grim, P. Andersson, A. Volodin, C. van Haesendonck, M. V. Auweraer, W. R. Salaneck and M. Berggren, *Chem. Mater.*, 2006, **18**, 4354; (*d*) A. M. Nardes, M. Kemerink, M. M. de Kok, E. Vinken, K. Maturova and R. A. J. Janssen, *Org. Electron.*, 2008, **9**, 727; (*e*) L. A. A. Pettersson, S. Ghosh and O. Inganäs, *Org. Electron.*, 2002, **3**, 143.
31 A. Borghese, G. Geldhof and L. Antoine, *Tetrahedron Lett.*, 2006, **47**, 9249.
32 J. Sinha, R. Sahoo and A. Kumar, *Macromolecules*, 2009, **42**, 2015.
33 A. Kumar and A. Kumar, *Polym. Chem.*, 2010, **1**, 286.
34 S. H. Baxamusa, S. G. Im and K. K. Gleason, *Phys. Chem. Chem. Phys.*, 2009, **11**, 5227.
35 A. S. Sarac, M. Ates and E. A. Parlak, *Appl. Electrochem.*, 2006, **36**, 889.

